Title
Enzymes and Models

ISBN
978-3-319-82928-9

Authors
Yachandra, VK
Yano, J

Publication Date
2017

Peer reviewed

Chapter 28
Enzymes and Models

Junko Yano and Vittal Yachandra

28.1 Introduction

Nature uses remarkably varied systems and mechanisms to perform chemical reactions with efficiency, speed, and complexity. At the active site of many enzymes are metal centers, responsible for the rearrangement of electrons and atoms in order to carry out electron transfer and catalytic reactions. Some of the representative metal clusters, especially those that contain heterometallic clusters, that are related to important reactions in nature, are shown in Fig. 28.1 [1–4]. Many of these consist of transition metals, such as V, Mn, Fe, Co, Ni, Cu, Zn, Mo, W and others. Using the flexibility of their electronic structures that can accommodate different redox states, they catalyze multi-electron reactions in aqueous solution, under conditions of ambient temperature and pressure.

Geometric and electronic structures of metal catalytic centers have been studied with X-ray absorption spectroscopy (XAS) in numerous metalloenzymes by taking advantage of the element-specificity of X-ray spectroscopy. X-ray absorption near edge spectroscopy (XANES) has been commonly used as a probe of the metal oxidation state, while extended X-ray absorption fine structure (EXAFS) has been applied for identifying the geometric structure of the metal complexes, and the method does not require single crystals. This makes the EXAFS method a powerful tool for extracting structural information of reaction intermediates, that cannot be crystallized. While solution NMR study is another way to get structural information of non-crystalline biological samples, it is difficult to apply the method to large metalloenzymes (>100 kDa) [5] or to study paramagnetic metal centers of metalloenzymes.

J. Yano (✉) • V. Yachandra
Molecular Biophysics and Integrated Bioimaging Division, Lawrence Berkeley National Laboratory, Berkeley, CA 94720, USA
e-mail: JYano@lbl.gov

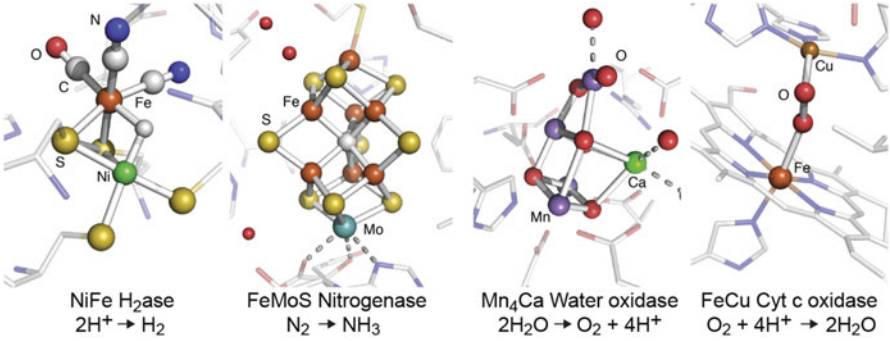

Fig. 28.1 Some examples of metalloenzymes that contain heterometallic clusters, such as NiFe hydrogenase, FeMo nitrogenase, Mn_4Ca water oxidase, and FeCu cytc oxidase, that have been studied using X-ray spectroscopic techniques

In addition to XAS, more advanced X-ray-based techniques such as RIXS (resonant inelastic X-ray scattering), XES (X-ray emission spectroscopy), and X-ray Raman spectroscopy [6], have been introduced to study biological systems, owing to the availability of bright synchrotron X-ray sources. XAS and XES data collection of biological samples have become somewhat routine. However, getting useful data often remains challenging due to several difficulties that are unique to biological systems. For example, X-ray-induced changes during data collection have been a concern. Reducing the background signal that arise from light atoms is another issue. Furthermore, interpreting X-ray spectroscopic data of biological systems often requires a set of adequate model complexes, that provide the basis for evaluating the influence of the coordination environment of the absorber elements. Study of structurally well-characterized model complexes also provides a benchmark for understanding the EXAFS from metal systems of unknown structures.

In this chapter, the X-ray spectroscopy methods that have been used for studying biological samples are described, using several examples. In addition to the synchrotron X-ray-based methods, recent introduction of XFELs (X-ray free electron lasers) have opened a new way of collecting X-ray spectroscopy of biological systems by capturing reaction intermediates under physiological conditions, and this chapter touches on some of the applications that have been demonstrated recently.

28.2 X-Ray Spectroscopy of Biological Systems

X-ray crystallography and X-ray spectroscopy of metalloenzymes provide complementary information: crystallography probes the structural changes of the cofactor and the overall protein, while XAS provides detailed information about changes in

the electronic structure of the metal of interest and its local structural information. When combined, these complementary measurements will provide a more detailed understanding of important enzymatic reactions.

In general, the advantage of EXAFS over X-ray crystallography is that the local structural information around the metal of interest can be obtained even from disordered samples such as powders and solution, and usually the metal–metal and metal–ligand distance information is much better than that can be obtained from crystallography. However, ordered samples like oriented membranes and single crystals often increase the information obtained from X-ray spectroscopy. The advantages and the limitations of XAS for the structural studies of biological systems are summarized in detail below.

1. In a metalloenzyme with multiple metal centers like cytochrome oxidase (Cu and Fe), photosystem II (Mn and Ca), or nitrogenase (Fe/V and Mo), it is possible to study the structural environment of each metal atom independently, because of the element specificity of XAS.
2. The metal of interest is never "*silent*" with respect to X-ray spectra, and one can always probe the metal site structure by X-ray spectroscopy. It could be "*silent*" with respect to EPR (electron paramagnetic resonance spectroscopy), optical, or other spectroscopic methods. However, this could become a disadvantage, if there are several metal centers going through different chemical states.
3. X-ray spectroscopy is not limited by the state of the sample, because it is sensitive only to the local metal site structure. Therefore, one can either trap intermediates in the enzymatic cycle or modify the site by the addition of inhibitors or substrate, or generate other chemical modifications or site-directed mutations. Such samples can be made as frozen solutions, avoiding the problems of trying to obtain single crystals.

It is also important to realize the intrinsic limitations of EXAFS for studying structures. A frequent problem is the inability to distinguish between scattering atoms with little difference in atomic number (C, N, O or S, Cl, or Mn, Fe). Distances are usually the most reliably determined structural parameters from EXAFS. But the range of data that can be collected, often-times due to practical reasons like the presence of the K-edge of another metal, or data collection time for dilute biological samples, limits the resolution of distance determinations to between 0.1 and 0.2 Å. Also it is difficult to determine whether a Fourier peak should be fit to one distance with a relatively large disorder parameter or to two distances, each having a small disorder parameter. Careful statistical analysis, taking into consideration the degrees of freedom in the fits, should precede any such analysis. The resolution in the distance Δr can be estimated from the relation that $\Delta r \Delta k \sim 1$ (see Sect. 4.2). Determination of coordination numbers or number of backscatterers is fraught with difficulties. The Debye-Waller factor is strongly correlated with the coordination number and one must have recourse to other information to narrow the range that is possible from curve fitting analysis alone.

It is therefore very useful to compare the spectra from the complex in the metalloenzyme to some known model complexes and then use Debye-Waller parameters obtained from the model complexes in the fits.

28.3 Radiation-Induced Changes During Data Collection

Damage to biological samples by X-rays is cause for serious concern for X-ray based experiments, in particular for the study of biological samples. However, with the right precautions one can successfully perform these experiments under the threshold of radiation damage. At synchrotron sources, most of the damage is produced by free radicals and hydrated electrons that are produced by X-rays in biological samples. The diffusion of the free radicals and hydrated electrons can be minimized by the use of low temperatures. The use of a liquid He flow cryostat or liquid He cryostream, where the samples are at atmospheric pressure in a He gas atmosphere, has greatly reduced the risk of sample damage by X-rays. XAS experiments require a lower X-ray dose than X-ray crystallography, and radiation damage can be precisely monitored and controlled, thus allowing for data collection from an intact form of metal catalytic centers.

An example of the X-ray-induced changes is shown in Fig. 28.2. Solutions of Photosystem II (PSII) that consists of the $MnCaO_5$ catalytic center were exposed to various X-ray doses at 100 K, leading to reduction of 5, 10 or 25 %, of the Mn in the sample from the native Mn(III,IV) to Mn(II) [7]. The corresponding XANES spectra are shown in Fig. 28.2a. A clear shift in the K-edge toward lower energies, due to the reduction to Mn(II) can be seen when comparing with the intact state

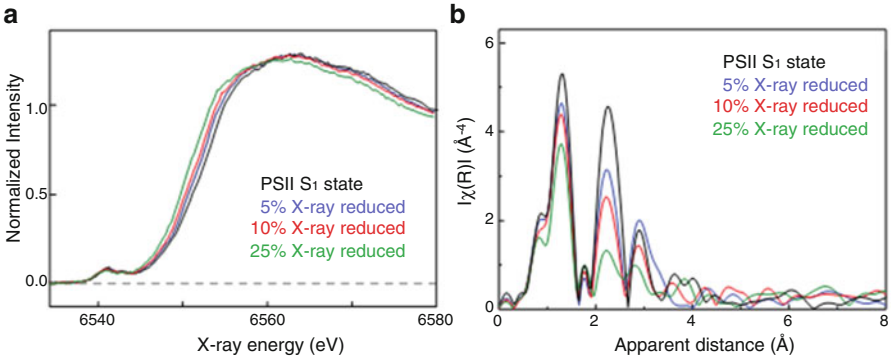

Fig. 28.2 (**a**) The Mn XANES spectrum of the oxygen-evolving complex from PS II that has been photo-reduced by X-rays to different levels between 5 and 25 %, compared to a spectrum from an intact PS II sample. (**b**) The corresponding Mn EXAFS Fourier transforms from the same PS II samples, showing the disruption of the Mn_4Ca oxo-bridged complex following X-ray radiation induced reduction. This disruption manifests itself as a decrease in the intensity of FT peaks assigned to Mn-Mn interactions at ~2.7 Å and/or Mn–Mn/Mn–Ca interactions at 3.2 Å [7]

spectrum from the native Mn(III,IV) form. In the EXAFS spectra (Fig. 28.2b), the intensities of all three peaks are decreased upon Mn reduction, with the most pronounced decrease in the second peak intensity, showing that upon Mn reduction Mn-Mn distances change and they are elongated. The reduction of the metal center by X-rays does not necessarily go through the catalytic reduction pathway, as it is likely caused by the random attack of hydroxyl radicals that are created by the interaction of X-rays and water molecules. Similar observations have been made in many Fe-containing proteins such as putidaredoxin [8], Cytochrome C peroxidase [9], and Fe/Fe and Fe/Mn ribonucleotide reductase [10], where the states generated by X-ray photoreduction are significantly different from the native catalytic state of the metal center. These studies show that radiation-induced changes are a general problem when studying metalloenzymes with X-rays. Such radiation-induced effects could potentially be turned into a tool to obtain new insights into the structural and electronic structural nature of the metal cluster.

Nevertheless, radiation-induced changes remain one of the most challenging aspects in biological X-ray spectroscopy. New approaches to overcome such effects and collect radiation-damage-free data have become possible, using XFELs which is described in Sect. 5.

28.4 Application of Various X-Ray Spectroscopy Techniques to Study Metalloenzymes

28.4.1 Polarized X-Ray Absorption Spectroscopy

As described above, the advantage of XAS is that the local structural information around the element of interest can be obtained from disordered samples such as powders and solutions. However, ordered samples like membranes and single crystals often increases the information obtained from XAS. For oriented single crystals or ordered membranes the interatomic vector orientations can be deduced from dichroism measurements.

Membrane proteins can be oriented on a substrate such that the lipid membrane planes are roughly parallel to the substrate surface. This imparts a one-dimensional order to these samples; while the z-axis for each membrane (collinear with the membrane normal) is roughly parallel to the substrate normal, the x- and y-axes remain disordered. Exploiting the plane-polarized nature of synchrotron radiation, spectra can be collected at different angles between the substrate normal and the X-ray E vector (Fig. 28.3a). The dichroism, which is the dependence of the intensity of the absorber–backscatterer pair present in the oriented samples as a function of the polarization of the X-rays, is reflected in, and can be extracted from, the resulting X-ray absorption spectra [11–13]. The EXAFS of the oriented PS II samples exhibits distinct dichroism, from which one can deduce the relative

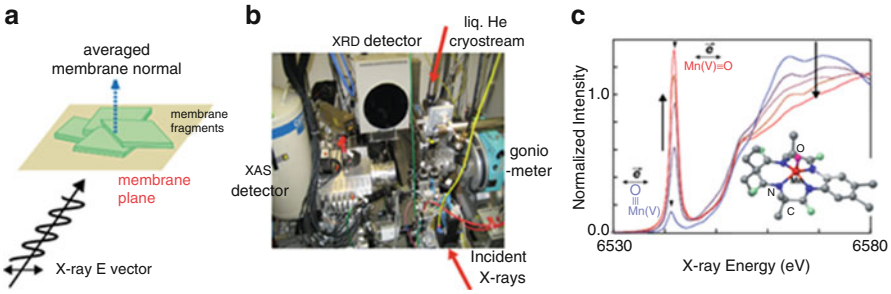

Fig. 28.3 (**a**) Experimental setup for single crystal X-ray absorption spectroscopy at the BL9-3 in SSRL. (**b**) Schematic picture of the polarized XAS data collection from 1D oriented membrane fragments. (**c**) Single crystal XAS of a Mn(V) inorganic complex, showing the pronounced dichroism of the XANES spectrum [11]

orientations of several interatomic vector directions relative to the membrane normal and derive a topological representation of the metal sites in the OEC [14].

Further refinement can be performed for samples with three-dimensional order. Figure 28.3b shows the experimental setup for collecting single crystal XAS data at the Stanford Synchrotron Radiation Lightsource, BL 9-3. It consists of a kappa goniometer, a 30-element Ge detector for collecting XAS data, and a 2D detector placed behind the sample for in situ collection of diffraction data to determine the crystal orientation. The crystals are cooled using a liquid He cryostream to minimize the radiation-induced changes of the sample. Single-crystal X-ray spectroscopy has been performed on model complexes [15] and metalloproteins [16–19]. These studies have been able to significantly expand the XAS information available for these systems over what is gleaned from studies of isotropic samples.

An example of polarized XANES spectra from a Mn(V) model complex is shown in Fig. 28.3c [11]. In this study, the orientationally resolved pre-edge peaks were correlated to DFT calculations, and the results were used for assigning the 1s to 3d transition components. The method was also applied to PSII in the dark state prior to the determination of high-resolution X-ray crystal structure, and the study improved the resolution and orientation of the metal–metal distances in EXAFS [17].

28.4.2 Range-Extended EXAFS

In the typical EXAFS measurement of biological samples, spectra are taken up to ~ 500 eV above the K-absorption edge, that provides a k-range of ~12.0 /Å. However, longer the *k*-range, the EXAFS distance resolution improves and it becomes important for some systems to resolve distance heterogeneity with similar

metal–ligand and metal–metal interactions. The distance resolution in a typical EXAFS experiment is given by

$$\Delta R = \pi / 2k_{\max} \tag{28.1}$$

where $k_{\max}$ is the maximum energy of the photoelectron of the absorber element.

Getting larger $k_{\max}$ is not always possible, in particular, for systems which contain adjacent elements in the periodic table due to the presence of the rising edge of the next element. In principle, solid-state detectors can be used for discriminating fluorescence signals from different elements, by electronically windowing the Kα fluorescence from the absorber atom and collecting XAS data as an excitation spectrum. However, the energy resolution of the detector at the transition metal absorption edges is about 150–200 eV (fwhm), and this makes it difficult to discriminate signals from adjacent transition metals. For the Mn K-edge EXAFS studies of PS II, for example, the absorption edge of the obligatory Fe in PS II (2-3Fe/PS II) limits the EXAFS energy range (Fig. 28.4). The use of a high-resolution crystal monochromator provides a method to selectively separate the fluorescence signals from adjacent metals, resulting in the collection of data to higher photoelectron energies and leading to increased distance resolution and more precise determination in the numbers of metal–metal vectors.

28.4.3 X-Ray Emission Spectroscopy

A complementary technique to XAS is XES. The photons that are emitted after the creation of a core hole in the 1s shell form the K emission spectrum. Among such emission processes, Kα lines originate from 2p to 1s transitions and Kβ lines from the 3p to 1s transitions ($K\beta_{1,3}/K\beta'$) and valence level to 1s transitions ($K\beta_{2,5}/K\beta''$)

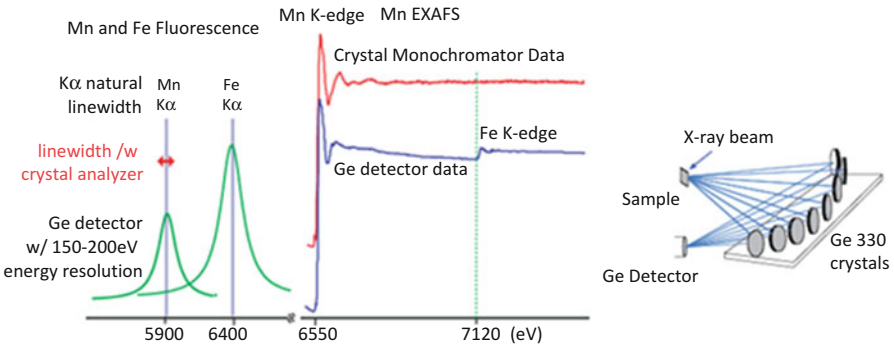

Fig. 28.4 (*left*) X-ray fluorescence of Mn and Fe. The multi-crystal monochromator with 1 eV resolution is tuned to the Mn $K\alpha_1$ peak. (*middle*) Traditional XAFS spectrum (*blue*) and using a crystal monochromator (*red*) (note the absence of Fe contribution). (*right*) The schematic for the crystal monochromator used in a backscattering configuration [14]

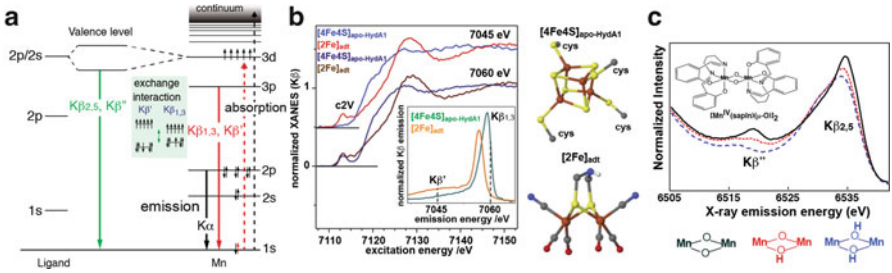

Fig. 28.5 (**a**) Energy level diagram showing the excitation and emission processes for the Kα, $K\beta_{1,3}$/Kβ′ and the $K\beta_{2,5}$/Kβ″ transitions. (**b**) Kβ-detected XAS of apo-HydA1 protein binding only the [4Fe4S] unit of the H-cluster and of a synthetic [2Fe] model complex. The *inset* shows the Kβ XES, and two detection energy for the XAS (7045 and 7060 eV) are shown as *dotted lines* in the *inset*. The figure was adapted from Ref. [20]. (**c**) The valence to core $K\beta_{2,5}$/Kβ″ emission spectra of a series of dinuclear Mn^{IV} complexes, where the bridging oxygen was protonated sequentially [21]

(Fig. 28.5a). These spectra change depending on the chemical environment of the metals of interest. In particular, Kβ spectra have been used in biological systems for probing the oxidation states and identifying the ligand environment.

$K\beta_{1,3}$/Kβ′ spectra arise predominantly from the exchange interaction between the metal 3p and the net electron spin in the metal valence shell, i.e., the effective number of unpaired metal 3d electrons. Therefore, the spectrum is sensitive to the spin state of the metals, which indirectly reflects the oxidation state and covalency of the metal site, and has often been used for determining the oxidation states of metal catalytic sites [6]. $K\beta_{1,3}$ arises from the constructive spin interactions, while Kβ′ from destructive spin interactions.

The sensitivity of the $K\beta_{1,3}$/Kβ′ spectra to the number of unpaired 3d electrons has the potential for being used for probing different metal sites in multinuclear clusters. As mentioned in Section II, there is no "silent" state in XAS. This can be a limiting factor for studying the system that contains several of the same element. For uniquely probing one particular reaction site, the use of different K-emission signals could become useful. One example is the [FeFe]-hydrogenases that contain 6 Fe in the metal catalytic center (H-cluster). Haumann et al. studied the H-cluster with site-selective XAS method, by using the $K\beta_{1,3}$ and Kβ′ signals to distinguish between the low and high spin Fe sites in the two subcomplexes (Fig. 28.5b) [20]. By using a high-resolution spectrometer, in one case the Kβ-detected XAS was collected at the Kβ′ energy and in the other case at the $K\beta_{1,3}$ energy; the former one represents the 2Fe site, while the latter one represents the 4Fe4S site. Thus the response of the two sites in different chemical states can be separately analyzed.

The higher energy emission peaks above $K\beta_{1,3}$ originate from valence-to-core transitions just below the Fermi level and can be separated into Kβ″ and the $K\beta_{2,5}$ emission (Fig. 28.5a). $K\beta_{2,5}$ emission is predominantly from ligand 2p (metal 4p) to metal 1s, and the Kβ″ emission is assigned to a ligand 2s to metal 1s; both are referred to as cross-over transitions [6]. Therefore, only direct ligands to the metal of interest are probed with $K\beta_{2,5}$/Kβ″ emission, i.e., other C, N, and O atoms in the

protein media do not contribute to the spectra. In particular, the energy of the Kβ″ transition depends on the difference between the metal 1s and ligand 2s binding energies, which reflects the environment of the ligand owing to orbital hybridization.

Detecting the chemical states of ligands is important for understanding the reaction mechanism of numerous metalloenzymes. In particular, protonation/deprotonation states of ligands moderate reaction chemistry in metal centers in biologically important processes. For example, copper oxo/hydroxo/peroxo complexes play vital roles in respiration, such as in hemocyanin [22], in biological metabolic pathways such as catechol oxidase activity or activation of aliphatic C-H bonds by dopamine β-monooxygenase [23], peptidyl-glycine α-amidating enzyme, and particulate methane monooxygenase [24]. It is also known that FeFe clusters in methane monooxygenase catalyze the hydroxylation of methane to methanol [25]. Understanding these events requires techniques that are sensitive enough to differentiate species that differ only by a single proton. Fig. 28.5c shows how the $K\beta_{2,5}$ and Kβ″ spectra change depending on the protonation state of the bridging oxygen ligands of the metal cluster [21]. Several techniques have the potential to detect such a single protonation event, that includes vibrational spectroscopy and ligand sensitive EPR techniques such as ENDOR (electron nuclear double resonance), ESEEM (electron spin echo envelope modulation), and HYSCORE (hyperfine sub-level correlation). The advantage of X-ray-based methods over EPR techniques is their element specificity and that they are unrestricted by the spin states of the compounds.

The $K\beta_{2,5}$ and Kβ″ XES was also applied for the study of nitrogenase to identify the central atom of the FeMoco cluster [26], using the element sensitivity of the Kβ″ peak position. A combination of the detailed data analysis and the theoretical calculations revealed that the central atom is a carbon.

28.4.4 Resonant Inelastic X-Ray Scattering Spectroscopy

The pre-edge region of metal K-edge XAS, that corresponds to the 1s to 3d transition, is a probe of metal oxidation state and local geometry of metal catalytic centers. However, the K pre-edge spectra are usually weak compared to the K-main edge, as they mostly arise from quadrupole transition matrix elements. In addition, it suffers from a strong background from the dipole-allowed transition of the main edge, particularly for early transition metals. Transition metal L-edge XAS are in some ways a superior chemical probe to K-edge spectra as (1) $2p \rightarrow 3d$ transitions are allowed under dipole selection rules, while only $s \rightarrow p$ transitions are allowed at the K-edge, (2) greater sensitivity to the occupancy of the 3d orbitals of metal provides a better indication of the oxidation states and symmetry of the complex involved. It is therefore anticipated that examination of the L-edge region will provide oxidation state information of the metal centers with significantly better resolution than that from K-edges. However, the disadvantage is that the energy of

these transitions requires the use of soft X-rays for direct excitation, leading to drastically increased radiation damage compared to high energy hard X-rays (100 times higher) and only surface absorption for bulk samples. These issues make soft X-ray (metal L-edge) spectroscopy less applicable to biological systems.

The above-described problems can be overcome in 1s2p RIXS (resonant inelastic X-ray scattering spectroscopy. In this method, hard X-rays tuned to the energy of the K pre-edge are used to excite a 1s electron into an unoccupied valence orbital (1s to 3d transition), and the emission due to decay of a 3p or 2p electron into the 1s shell is measured as a function of the excitation energy. In experiments, the incident energy is varied across the metal K-edge (1s to 3d) using hard X-rays, and the crystal analyzer is scanned over the Kα emission energy (2p to 1s). The energy difference between excitation and emission corresponds to the energy difference between 2p or 3p and 3d orbitals and, therefore, one can get L-edge-like XAS spectrum while taking advantage of using hard X-rays (high-excitation energy and therefore the high X-ray penetration depth and larger attenuation length) to probe these transitions indirectly. In addition, the RIXS 2D plot also makes the background separation of the pre-edge structure from the main K-edge feature easier.

As an example, the Fe site of the cytochrome c (cyt c) and its model compound was studied by Fe 1s2d RIXS [27]. The RIXS study was used to quantify the highly covalent nature of the porphyrin environment in the heme cofactor, through the analysis of the L-edge XAS-like data from RIXS, and showed the increased covalency for the Fe-S(Met) relative to Fe-N(His) axial ligand and a higher degree of covalency for the ferric states relative to the ferrous states. Namely, it suggests that the bond strengths for the Fe(II) and Fe(III) states are a critical factor for the enzymatic function.

28.5 Application of XFELs for the Study of Metalloenzymes Using X-Ray Spectroscopy

X-ray based techniques, such as X-ray spectroscopy, X-ray crystallography, as well as X-ray scattering methods, have contributed significantly to the structural and functional studies of metalloenzymes in the last decades, and have become indispensable methods. However, to minimize or eliminate radiation-induced changes during data collection has remained challenging. As described in Section II, the data collection of biological samples is usually carried out at cryogenic temperature to minimize the X-ray induced effect. However, there is an increasing effort to understand biological phenomena as the enzymes function, through studies under physiological/functional conditions. Additionally, the need to probe rare transitions, which often are superior probes of chemical states but require very high photon fluxes, , within a reasonable time, is another issue.

The recent advent of XFELs [28, 29] brought the possibility of probing labile biological systems with high dose X-rays, by outrunning the radiation damage

processes and extracting the information before manifestation of the X-ray-induced changes to the sample using fs X-ray pulses. XFELs produce high intensity X-ray pulses in the fs time regime. In practice the number of photons in a single <50 fs pulse is comparable to the number of photons available per second in a modern third generation synchrotron end station. In addition to serial femtosecond crystallography (e.g., Ref. [30]), X-ray spectroscopic techniques have been applied for the study of metalloenzymes at the XFELs, and have shown promise. Both XAS and XES methods are currently targeted at XFEL sources.

The hard X-ray XES method has a few advantages, when it is applied at the XFELs. No monochromatization is necessary and the full SASE (self-amplified spontaneous emission) bandwidth of the XFEL pulse can be used in the shot-by-shot data collection [31–33]. Kβ XES on dilute solution samples was initially demonstrated for Mn compounds [31], showing that the fs pulses used did not disturb the electronic structure of the compounds studied (Mn^{II} and $Mn^{III,IV}$). For iron(II) tris(2,2′-bipyridine) it was also possible to record time resolved XES at 50 fs to 1 ps after a laser excitation and resolve the kinetics of the light-induced spin change using 50 mM concentration in a 100 μm thick liquid jet. An XAS method was also used at XFELs for pump-probe measurements [34], providing unique insights into the evolution of the electronic structure over the reaction cycle. In addition to hard X-ray spectroscopy, XFELs provide a new opportunity to carry out biological soft X-ray spectroscopy [35] by overcoming severe radiation damage due to the high absorption cross section at the soft X-ray energy range, that has been an issue in the synchrotron X-ray sources.

Among the several X-ray spectroscopic methods, XES is well suited to be combined with other techniques. For example, XES can be collected simultaneously with X-ray crystallography by choosing the same excitation energy (Fig. 28.6). Such a method was developed and used for studying the water oxidation reaction in PS II with microcrystals [36]. In this approach, XES provides a diagnostic capability by providing the electronic structure of the highly radiation sensitive Mn_4CaO_5 cluster in PS II. Furthermore, it serves for monitoring the catalytic turn over under the experimental conditions.

28.6 Future Direction

X-ray spectroscopy, together with X-ray crystallography, has been an extremely important method for understanding the mechanism of metal catalytic reactions in metalloenzymes. The development of theoretical approaches, like density functional theory (DFT), with well-characterized model inorganic complexes has provided the necessary information for interpreting spectroscopic data. Furthermore, the recent development of bright synchrotron X-ray sources and the X-ray free electron laser further opens new horizons for data collection from biological samples under physiological conditions in a time-resolved manner. These developments altogether will provide tools for us to understand the mechanism of catalytic

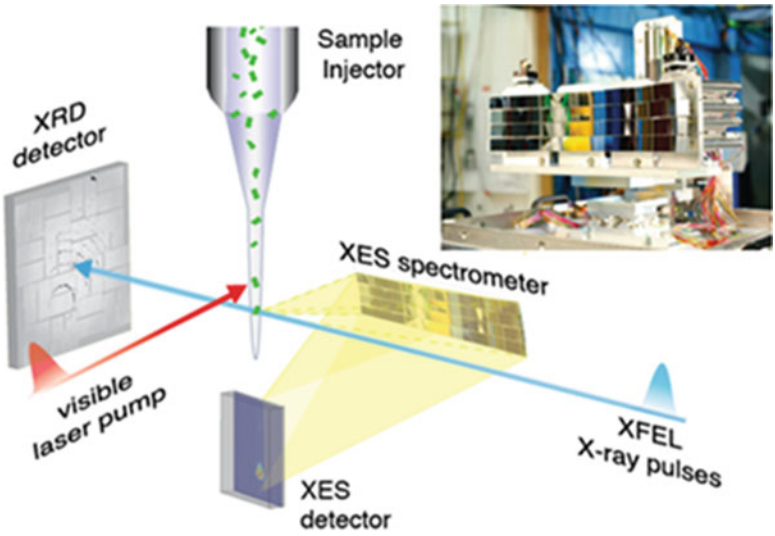

Fig. 28.6 Setup for simultaneous XES/XRD at the LCLS XFEL. The XES spectrometer is mounted at 90° to the fs X-ray pulses and the XRD is recorded in forward scattering. The sample is introduced into the interaction region using a jet as shown here, but other methods can also be used. The energy dispersive XES spectrometer is shown at *top right*. Illumination of the samples is achieved by visible laser pumps and are used for time resolved optical pump X-ray probe measurements [36]

reaction paths in metalloenzymes and the important information of how to control electron/proton flow and product/substrate transport, spatially and temporally, during catalysis using the protein framework.

References

1. Ogata H, Nishikawa K, Lubitz W (2015) Hydrogens detected by subatomic resolution protein crystallography in a [NiFe] hydrogenase. Nature 520:571
2. Kaiser JT, Hu Y, Wiig JA, Rees DC, Ribbe MW (2011) Structure of precursor-bound NifEN: a nitrogenase femo cofactor maturase/insertase. Science 331:91
3. Suga M, Akita F, Hirata K, Ueno G, Murakami H, Nakajima Y, Shimizu T, Yamashita K, Yamamoto M, Ago H, Shen J-R (2015) Native structure of photosystem II at 1.95 Å resolution viewed by femtosecond X-ray pulses. Nature 517:99
4. Tsukihara T, Aoyama H, Yamashita E, Tomizaki T, Yamaguchi H, Shinzawa-Itoh K, Nakashima R, Yaono R, Yoshikawa S (1995) Structures of metal sites of oxidized bovine heart cytochrome c oxidase at 2.8 Å. Science 269:1069
5. Tzakos AG, Grace CRR, Lukavsky PJ, Riek R (2006) NMR techniques for very large proteins and RNAs in solution. Annu Rev Biophys Biomol Struct 35:319
6. Glatzel P, Bergmann U (2005) High resolution 1s core hole X-ray spectroscopy in 3d transition metal complexes - electronic and structural information. Coord Chem Rev 249:65

7. Yano J, Kern J, Irrgang K-D, Latimer MJ, Bergmann U, Glatzel P, Pushkar Y, Biesiadka J, Loll B, Sauer K, Messinger J, Zouni A, Yachandra VK (2005) X-ray damage to the Mn4Ca complex in single crystals of photosystem II: a case study for metalloprotein crystallography. Proc Natl Acad Sci U S A 102:12047
8. Corbett MC, Latimer MJ, Poulos TL, Sevrioukova IF, Hodgson KO, Hedman B (2007) Photoreduction of the active site of the metalloprotein putidaredoxin by synchrotron radiation. Acta Cryst 63:951
9. Meharenna YT, Doukov T, Li HY, Soltis SM, Poulos TL (2010) Crystallographic and single-crystal spectral analysis of the peroxidase ferryl intermediate. Biochemistry 49:2984
10. Sigfridsson KGV, Chernev P, Leidel N, Popović-Bijelić A, Gräslund A, Haumann M (2013) Rapid X-ray photoreduction of dimetal-oxygen cofactors in ribonucleotide reductase. J Biol Chem 288:9648
11. Yano J, Robblee J, Pushkar Y, Marcus MAM, Bendix J, Workman JM, Collins TJ, Solomon EI, George SD, Yachandra VK (2007) Polarized X-ray absorption spectroscopy of single-crystal Mn(V) complexes relevant to the oxygen-evolving complex of photosystem II. J Am Chem Soc 129:12989
12. George GN, Prince RC, Frey TG, Cramer SP (1989) Oriented X-ray absorption-spectroscopy of membrane-bound metalloproteins. Physica B 158:81
13. George GN, Cramer SP, Frey TG, Prince RC (1993) X-ray-absorption spectroscopy of oriented cytochrome-oxidase. Biochim Biophys Acta 1142:240
14. Pushkar Y, Yano J, Glatzel P, Messinger J, Lewis A, Sauer K, Bergmann U, Yachandra VK (2007) Structure and orientation of the Mn Ca cluster in plant photosystem II membranes studied by polarized range-extended X-ray absorption spectroscopy. J Biol Chem 282:7198
15. Pickering IJ, George GN (1995) Polarized X-ray-absorption spectroscopy of cupric chloride dihydrate. Inorg Chem 34:3142
16. Flank AM, Weininger M, Mortenson LE, Cramer SP (1986) Single-crystal EXAFS of nitrogenase. J Am Chem Soc 108:1049
17. Yano J, Kern J, Sauer K, Latimer M, Pushkar Y, Biesiadka J, Loll B, Saenger W, Messinger J, Zouni A, Yachandra VK (2006) Where water is oxidized to dioxygen: structure of the photosynthetic Mn Ca cluster. Science 314:821
18. George GN, Hilton J, Temple C, Prince RC, Rajagopalan KV (1999) Structure of the molybdenum site of dimethyl sulfoxide reductase. J Am Chem Soc 121:1256
19. Scott RA, Hahn JE, Doniach S, Freeman HC, Hodgson KO (1982) Polarized X-ray absorption-spectra of oriented plastocyanin single-crystals - investigation of methionine copper coordination. J Am Chem Soc 104:5364
20. Chernev P, Lambertz C, Brunje A, Leidel N, Sigfridsson KG, Kositzki R, Hsieh CH, Yao S, Schiwon R, Driess M, Limberg C, Happe T, Haumann M (2014) Hydride binding to the active site of [FeFe]-hydrogenase. Inorg Chem 53:12164
21. Lassalle-Kaiser B, Boron TT 3rd, Krewald V, Kern J, Beckwith MA, Delgado-Jaime MU, Schroeder H, Alonso-Mori R, Nordlund D, Weng TC, Sokaras D, Neese F, Bergmann U, Yachandra VK, DeBeer S, Pecoraro VL, Yano J (2013) Experimental and computational X-ray emission spectroscopy as a direct probe of protonation states in Oxo-bridged Mn dimers relevant to redox-active metalloproteins. Inorg Chem 52:12915
22. Magnus KA, Tonthat H, Carpenter JE (1994) Recent structural work on the oxygen-transport protein hemocyanin. Chem Rev 94:727
23. Klinman J (2006) The copper-enzyme family of dopamine β -monooxygenase and peptidylglycine α-hydroxylating monooxygenase: resolving the chemical pathway for substrate hydroxylation. J Biol Chem 281:3013
24. Himes RA, Karlin KD (2009) Copper-dioxygen complex mediated C-H bond oxygenation: relevance for particulate methane monooxygenase (pMMO). Curr Opin Chem Biol 13:119
25. Kryatov SV, Taktak S, Korendovych IV, Rybak-Akimova EV, Kaizer J, Torelli S, Shan XP, Mandal S, MacMurdo VL, Payeras AMI, Que L (2005) Dioxygen binding to complexes with

Fe (μ-OH) cores: steric control of activation barriers and O -adduct formation. Inorg Chem 44:85
26. Lancaster KM, Roemelt M, Ettenhuber P, Hu Y, Ribbe MW, Neese F, Bergmann U, DeBeer S (2011) X-ray emission spectroscopy evidences a central carbon in the nitrogenase iron-molybdenum cofactor. Science 334:974
27. Kroll T, Hadt RG, Wilson SA, Lundberg M, Yan JJ, Weng TC, Sokaras D, Alonso-Mori R, Casa D, Upton MH, Hedman B, Hodgson KO, Solomon EI (2014) Resonant inelastic X-ray scattering on ferrous and ferric bis-imidazole porphyrin and cytochrome c: nature and role of the axial Methionine-Fe bond. J Am Chem Soc 136:18087
28. Emma P, Akre R, Arthur J, Bionta R, Bostedt C, Bozek J, Brachmann A, Bucksbaum P, Coffee R, Decker FJ, Ding Y, Dowell D, Edstrom S, Fisher A, Frisch J, Gilevich S, Hastings J, Hays G, Hering P, Huang Z, Iverson R, Loos H, Messerschmidt M, Miahnahri A, Moeller S, Nuhn HD, Pile G, Ratner D, Rzepiela J, Schultz D, Smith T, Stefan P, Tompkins H, Turner J, Welch J, White W, Wu J, Yocky G, Galayda J (2010) First lasing and operation of an Å-wavelength free-electron laser. Nat Photonics 4:641
29. Ishikawa T, Aoyagi H, Asaka T, Asano Y, Azumi N, Bizen T, Ego H, Fukami K, Fukui T, Furukawa Y, Goto S, Hanaki H, Hara T, Hasegawa T, Hatsui T, Higashiya A, Hirono T, Hosoda N, Ishii M, Inagaki T, Inubushi Y, Itoga T, Joti Y, Kago M, Kameshima T, Kimura H, Kirihara Y, Kiyomichi A, Kobayashi T, Kondo C, Kudo T, Maesaka H, Marechal XM, Masuda T, Matsubara S, Matsumoto T, Matsushita T, Matsui S, Nagasono M, Nariyama N, Ohashi H, Ohata T, Ohshima T, Ono S, Otake Y, Saji C, Sakurai T, Sato T, Sawada K, Seike T, Shirasawa K, Sugimoto T, Suzuki S, Takahashi S, Takebe H, Takeshita K, Tamasaku K, Tanaka H, Tanaka R, Tanaka T, Togashi T, Togawa K, Tokuhisa A, Tomizawa H, Tono K, Wu SK, Yabashi M, Yamaga M, Yamashita A, Yanagida K, Zhang C, Shintake T, Kitamura H, Kumagai N (2012) A compact X-ray free-electron laser emitting in the sub-Å region. NatPhotonics 6:540
30. Chapman HN, Fromme P, Barty A, White TA, Kirian RA, Aquila A, Hunter MS, Schulz J, DePonte DP, Weierstall U, Doak RB, Maia FRNC, Martin AV, Schlichting I, Lomb L, Coppola N, Shoeman RL, Epp SW, Hartmann R, Rolles D, Rudenko A, Foucar L, Kimmel N, Weidenspointner G, Holl P, Liang MN, Barthelmess M, Caleman C, Boutet S, Bogan MJ, Krzywinski J, Bostedt C, Bajt S, Gumprecht L, Rudek B, Erk B, Schmidt C, Homke A, Reich C, Pietschner D, Struder L, Hauser G, Gorke H, Ullrich J, Herrmann S, Schaller G, Schopper F, Soltau H, Kuhnel KU, Messerschmidt M, Bozek JD, Hau-Riege SP, Frank M, Hampton CY, Sierra RG, Starodub D, Williams GJ, Hajdu J, Timneanu N, Seibert MM, Andreasson J, Rocker A, Jonsson O, Svenda M, Stern S, Nass K, Andritschke R, Schroter CD, Krasniqi F, Bott M, Schmidt KE, Wang XY, Grotjohann I, Holton JM, Barends TRM, Neutze R, Marchesini S, Fromme R, Schorb S, Rupp D, Adolph M, Gorkhover T, Andersson I, Hirsemann H, Potdevin G, Graafsma H, Nilsson B, Spence JCH (2011) Femtosecond X-ray protein nanocrystallography. Nature 470:73
31. Alonso-Mori R, Kern J, Gildea RJ, Sokaras D, Weng TC, Lassalle-Kaiser B, Tran R, Hattne J, Laksmono H, Hellmich J, Glockner C, Echols N, Sierra RG, Schafer DW, Sellberg J, Kenney C, Herbst R, Pines J, Hart P, Herrmann S, Grosse-Kunstleve RW, Latimer MJ, Fry AR, Messerschmidt MM, Miahnahri A, Seibert MM, Zwart PH, White WE, Adams PD, Bogan MJ, Boutet S, Williams GJ, Zouni A, Messinger J, Glatzel P, Sauter NK, Yachandra VK, Yano J, Bergmann U (2012) Energy-dispersive X-ray emission spectroscopy using an X-ray free-electron laser in a shot-by-shot mode. Proc Natl Acad Sci U S A 109:19103
32. Zhang WK, Alonso-Mori R, Bergmann U, Bressler C, Chollet M, Galler A, Gawelda W, Hadt RG, Hartsock RW, Kroll T, Kjaer KS, Kubicek K, Lemke HT, Liang HYW, Meyer DA, Nielsen MM, Purser C, Robinson JS, Solomon EI, Sun Z, Sokaras D, van Driel TB, Vanko G, Weng TC, Zhu DL, Gaffney K (2014) Tracking excited-state charge and spin dynamics in iron coordination complexes. J Nature 509:345

33. Bertoni R, Cammarata M, Lorenc M, Matar SF, Letard JF, Lemke HT, Collet E (2015) Ultrafast light-induced spin-state trapping photophysics investigated in Fe(phen) (NCS) spin-crossover crystal. Acc Chem Res 48:774
34. Lemke HT, Bressler C, Chen LX, Fritz DM, Gaffney KJ, Galler A, Gawelda W, Haldrup K, Hartsock RW, Ihee H, Kim J, Kim KH, Lee JH, Nielsen MM, Stickrath AB, Zhang WK, Zhu DL, Cammarata M (2013) Femtosecond X-ray absorption spectroscopy at a hard X-ray free electron laser: application to spin crossover dynamics. J Phys Chem A 117:735
35. Mitzner R, Rehanek J, Kern J, Gul S, Hattne J, Taguchi T, Alonso-Mori R, Tran R, Weniger C, Schroder H, Quevedo W, Laksmono H, Sierra RG, Han G, Lassalle-Kaiser B, Koroidov S, Kubicek K, Schreck S, Kunnus K, Brzhezinskaya M, Firsov A, Minitti MP, Turner JJ, Moeller S, Sauter NK, Bogan MJ, Nordlund D, Schlotter WF, Messinger J, Borovik A, Techert S, de Groot FM, Fohlisch A, Erko A, Bergmann U, Yachandra VK, Wernet P, Yano J (2013) L-edge X-ray absorption spectroscopy of dilute systems relevant to metalloproteins using an X-ray free-electron laser. J Phys Chem Lett 4:3641
36. Kern J, Alonso-Mori R, Tran R, Hattne J, Gildea RJ, Echols N, Glockner C, Hellmich J, Laksmono H, Sierra RG, Lassalle-Kaiser B, Koroidov S, Lampe A, Han G, Gul S, Difiore D, Milathianaki D, Fry AR, Miahnahri A, Schafer DW, Messerschmidt M, Seibert MM, Koglin JE, Sokaras D, Weng TC, Sellberg J, Latimer MJ, Grosse-Kunstleve RW, Zwart PH, White WE, Glatzel P, Adams PD, Bogan MJ, Williams GJ, Boutet S, Messinger J, Zouni A, Sauter NK, Yachandra VK, Bergmann U, Yano J (2013) Simultaneous femtosecond X-ray spectroscopy and diffraction of photosystem II at room temperature. Science 340:491